Accelerating the magnetic island by the modulated resonant magnetic perturbation for the disruption avoidance on J-TEXT

Da Li[1], Nengchao Wang[1], Yonghua Ding[1,*], Qingquan Yu[2], Mao Li[3], Qiming Hu[4], Ying He[1], Feiyue Mao[1], Chengshuo Shen[1], Ruo Jia[1], Zhuo Huang[1], Song Zhou[1], Shuhao Li[1], Abba Alhaji Bala [1,5], Zhipeng Chen[1], Zhongyong Chen[1], Zhoujun Yang[1], Bo Rao[1], Zhonghe Jiang[1], Lin Yi[6], Kexun Yu[1], Yuan Pan[1] and J-TEXT team[1,†]

[1] International Joint Research Laboratory of Magnetic Confinement Fusion and Plasma Physics, State Key Laboratory of Advanced Electromagnetic Engineering and Technology, School of Electrical and Electronic Engineering, Huazhong University of Science and Technology, Wuhan 430074, People's Republic of China
[2] Max-Planck-Institut für Plasmaphysik, Garching 85748, Germany
[3] Laboratory of Low Frequency Electromagnetic Communication Technology with the Wuhan Maritime Communication Research Institute, China State Shipbuilding Corporation limited, Wuhan, 430205, People's Republic of China
[4] Princeton Plasma Physics Laboratory, Princeton, NJ 08543-0451, United States of America
[5] Physics Department, Federal University Dutse, Jigawa, Nigeria
[6] Department of Physics, Huazhong University of Science and Technology, Wuhan 430074, People's Republic of China
E-mail: yhding@hust.edu.cn

Abstract

The acceleration of the magnetic island rotation by the modulated resonant magnetic perturbation (MRMP) has been studied in J-TEXT tokamak experiments. After applying the MRMP, the phase difference between the TM and MRMP, $\Delta\xi$, oscillated near the effective phase difference, $\Delta\xi_{eff}$, which was defined as the time averaged value of $\Delta\xi$. When the $\Delta\xi_{eff}$ was closed to the $-\pi/2$, the MRMP only contributed an accelerating torque on the TM. As the result, the TM rotation frequency was increased by a few kilohertz for the optimized relative phase by small RMPs of the order of 10^{-5} of the toroidal field and the locked mode induced disruption was avoided. It's found that the TM rotation could be increased to a higher frequency by applying a stronger MRMP. There is a negative sinusoidal relationship between TM frequency and $\Delta\xi_{eff}$.

* E-mail: yhding@hust.edu.cn

† See Liang *et al* 2019 (https://doi.org/10.1088/1741-4326/ab1a72) for the J-TEXT team

1. Introduction

Tearing modes (TMs) or neoclassical tearing modes (NTMs) are one of the major performance limitation for tokamak plasmas[1, 2, 3]. Large magnetic islands, especially the islands with the poloidal/toroidal mode number m/n = 2/1, can slow down the plasma rotation by interacting with wall[4] or error field[5, 6] and even be locked, which is the main cause of the disruptions[7, 8]. Due to the low-torque input, the plasma rotation frequency is expected to be low in a fusion reactor. Low-m NTMs are predicted to be much more easily locked by the error field in a fusion reactor than in existing tokamaks, since the mode locking threshold is proportional to the mode frequency but inversely proportional to the square of the Alfven velocity [9]. Although rotating NTMs can be stabilized by localized electron cyclotron current drive (ECCD)[10, 11] or electron cyclotron resonance heating (ECRH)[12], once the island is locked at a certain phase by the error field, the island center will not necessarily be at the wave deposition region, and the mode stabilization by ECCD might become impossible. Therefore, it is very important to find an efficient way to maintain or to speed up the magnetic island rotation for avoiding mode locking in a fusion reactor [13, 14].

The dynamic resonant magnetic perturbations (RMPs) is an effective method to accelerate the TM due to the low requirement of RMP amplitude to speed up the rotation of a large island, especially for a fusion reactor [9]. The rotating RMPs with a higher frequency can be utilized to speed up TMs [15] and avoid the locked mode induced disruption [16]. But, it's difficult to accelerate TM with the rotating RMP when the frequency difference between them is too large. The TM also could be accelerated by a dynamic RMP with the increasing frequency [17]. When the frequency difference is too large, the TM unlocks from the increasing frequency dynamic RMP and returns to its initial frequency. In HBT-EP tokamak [17] and ACT tokamak [18], the phase shift dynamic RMP was used to accelerate the TM and a trigonometric relationship between the mode frequency and the shift phase was found in experiments. However, it's reported that phase instability could occur during the input of the phase shift RMP[19]. The phase instability was caused by the limited response time of the power supply and lead to the increase of TM amplitude. Hence, it's necessary to find a dynamic RMP strategy, which is easily realized in engineering and robust to avoid the phase instability. Meanwhile, the RMP with this strategy could continuously maintain a high TM rotation.

Based on the simulation investigation, the modulated RMP (MRMP), turning on the RMP only when the RMP contributes an accelerating torque , could accelerating the TM with a small amplitude [20]. In J-TEXT, the two groups RMP coils [21], with a toroidal spatial phase difference of 90˚, are feedback controlled independently [22]. In order to improve the utilization of RMP and eliminate the static component, the RMP coils are fed by bi-polar pulsed currents, which is positive for certain region and negative for the else region in experiments [23].The MRMP refers to applying the RMP only for a certain range of phase difference between the RMP and the island via feedback control. The experiments of controlling TM rotation with MRMP have been

carried out on J-TEXT tokamak. It is found that a small MRMP can effectively speed up a large island rotation. The TM frequency is accelerated from 4.3 kHz to 7 kHz by the MRMP and no phase instability occurred. The optimal phase difference to speed up the island rotation is found to be around $\Delta\xi = -\pi/2$. In a disruptive experimental condition, the MRMP maintains the TM rotation and prevents the mode locking. As a result, the disruption is avoided.

In section 2 our experimental set-up is described. The experimental results are presented in section 3. Finally, section 4 gives the discussion and conclusion.

2. Experimental Set-up

J-TEXT tokamak [24, 25] is a circular cross-section device (major radius R = 105 cm and minor radius a = 25.5 cm) with a movable limiter. For the experiments reported in this paper, the plasmas were operated with a = 25.5 cm, the toroidal field B_T = 1.6 T, plasma current I_p = 180 kA, line averaged electron density $n_e = 1.2 \sim 1.4 \times 10^{19} m^{-3}$, and edge safety factor $q_a \approx 2.7$. When the I_p reaches the flap top region, the m/n = 2/1 TM usually appears in these experiments, with the 2/1 island width being larger than 5cm (~20%a) and a frequency about 4 kHz.

The effect of the RMP on the TM depends on their relative phase difference [26, 27, 28], $\Delta\xi = \xi_{TM} - \xi_{RMP}$, where ξ_{TM} and ξ_{RMP} are the helical phase ($\xi = m\theta + n\varphi$) of the TM and the RMP. [15, 17, 29]. The electromagnetic (EM) torque applied to the plasma by RMPs is proportional to $B_{rmp}W^2\sin(\Delta\xi)$ [29], where B_{rmp} is the RMP amplitude, and W is the island width. The EM torque speeds up the island rotation for $\Delta\xi \in [-\pi, 0]$ but slows down the rotation for the opposite phase [29].

The applied MRMP are generated by 12 in-vessel saddle coils on J-TEXT [21]. These coils are divided into two groups, connected in a way to have a large m/n=2/1 component [30]. When applying DC coil currents, the RMP phases from the two groups coils differ about $\pi/2$. Based on the phase differences between RMP and the TM, two groups RMP coils are feedback controlled [31] and fed by bi-polar pulsed currents, which is positive for $\pi < \Delta\xi < 2\pi$ and negative for $0 < \Delta\xi < \pi$. The phase of TM was measured by magnetic probes and calculated in real-time [32]. The maximal RMP coil current is 2 kA, with the maximum frequency 8 kHz. Due to the eddy current in the wall, the amplitude of the 2/1 component of MRMP at the last closed flux surface decreases with increasing the RMP frequency. In the range of several kilohertz, however, the MRMP amplitude is about 0.39 Gs/kA and only slightly changes, as shown by figure 1 in reference [21].

The MRMP coil currents are shown for discharge #1059009 in Fig. 1 (b). The total MRMP rotates in the same direction as the mode rotation. Due to the limitation in the power supply system, the phase difference $\Delta\xi$ oscillates near the target value, as shown in Fig. 1 (c). The MRMP amplitude also oscillates, and the time-averaged value is around 0.64 Gs shown in Fig. 1 (d). Comparing with the phase shift dynamic RMP [17], only the direction of RMP current is feedback controlled for the MRMP, which decreases the requirement of the RMP power supply. In our experiments, no phase instability has been observed.

As the torque applied to the plasma from the MRMP is proportional to $\sin(\Delta\xi)$,

the utilization rate of the MRMP, κ_{eff}, can be assessed by

$$\kappa_{eff} = -\int_0^{\Delta t} B_{r,RMP}^{2/1}(t)\sin(\Delta\xi)dt \Big/ \int_0^{\Delta t} B_{r,RMP}^{2/1}(t)dt \qquad (1)$$

where $B_{r,RMP}^{2/1}$ is 2/1 component amplitude of the radial magnetic field generated by the MRMP , and Δt is the mode rotation period. In our experiments, the value of κ_{eff} is higher than 93%. The net EM torque could be described by the time-averaged torque in each period. Assuming a constant MRMP amplitude, the averaged torque is proportional to -sin ($\Delta\xi_{\text{eff}}$), where the effective phase difference $\Delta\xi_{\text{eff}}$ is defined by

$$\sin(\Delta\xi_{eff}) = \int_0^{\Delta t} \sin(\Delta\xi)dt / \Delta t \qquad (2)$$

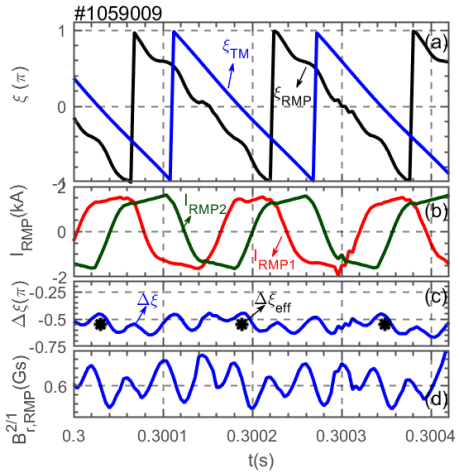

Fig. 1 From top to bottom, the time evolution of (a) the TM (blue line) and the MRMP phase (black line), (b) the currents of first (red line, 0.32 Gs/kA, $\xi_{RMP\,1}$ = 233˚) and second group coils (green line, 0.39 Gs/kA, ξ_{RMP2} = 143˚), (c) the phase difference, $\Delta\xi$, between the TM and the MRMP (blue curve) and the effective phase difference $\Delta\xi_{eff}$ (black asterisks), (d) the MRMP amplitude of the 2/1 component. The phase difference $\Delta\xi$ is around - 0.55 ± 0.1 π, and the effective phase difference $\Delta\xi_{eff}$ = -0.56 π.

3. Experimental Results

An example of preventing the disruption is shown in Fig. 2. Without MRMP, the TM frequency decreases at 0.29 s and the TM amplitude increases rapidly. The major disruption occurred once the TM rotation reaches zero as black curves in the Fig. 2. In the similar experimental condition, the MRMP ($B^{2/1}_{\text{r, RMP}}$ = 0.56 Gs, $\Delta\xi_{\text{eff}}$ = 1.7 π) was applied before mode locking at 0.23 s. After applying the MRMP, the TM frequency was increased from 4.5 kHz to the 5.5 kHz and the discharges were sustained during the region of applying MRMP. In the #1059012, the MRMP was turned down early at 0.313 s. The mode frequency decreased immediately after the decreases of MRMP amplitude. The TM amplitude increased with the decrease of mode frequency. The major disruption occurred when the TM was locked to the resistive wall, shown as the blue curves in the Fig. 2. When the MRMP was turned on continuously, the TM rotation was maintained 5.5 kHz by the MRMP, shown as the red curves in the Fig. 2.

As a results, the disruption was avoided in the #1059013.

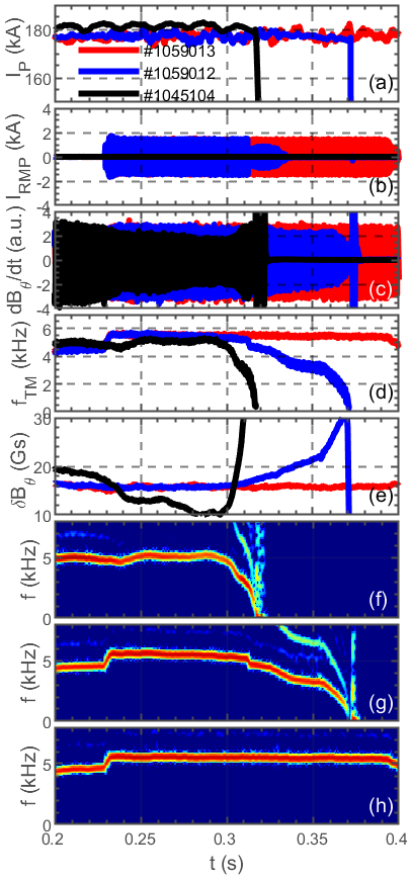

Fig. 2 Avoiding of disruption by using a MRMP (I_{RMP} = 1.4 kA, $B^{2/1}_{r,RMP}$ = 0.56 Gs, $\Delta\xi_{eff}$ = 1.7 π, red curves), compared to discharges with an early shutdown MRMP (blue curves) and without MRMP (black curves). From top to bottom: the time evolution of (a) plasma current, I_P, (b) the RMP current, I_{RMP}, (c) the Mirnov signal at the middle plane of the low field side, dB_θ/dt, (d) the TM frequency, f_{TM}, (e) the perturbed poloidal magnetic field generated by TM, δB_θ, and the spectrum of the Mirnov signal in (f) the without MRMP case, (g) the early shutdown MRMP case and (h) the disruption prevention case.

The TM rotation acceleration by the MRMP in discharge #1059009 is displayed in Fig. 3. The MRMP was applied from 0.23 s, and its amplitude was ramped up to 0.64 Gs in 6 ms, as shown in Fig. 3(a). Fig. 3(b) shows the value of $\Delta\xi_{\text{eff}}$. After applying the MRMP, the instantaneous frequency of TM was not a constant in a rotation period. The time evolution of TM frequency is described by the averaged frequency f_{ave} in each period (blue points in Fig. 3(c)). The MRMP frequency (black points in Fig. 3 (c)) followed the TM frequency via feedback control. The TM frequency was increased immediately once the MRMP was applied, with an increasing rate about ~ 400 kHz/s. After t=0.24 s, the TM frequency was maintained around 6.3 kHz by the MRMP. The phase difference $\Delta\xi$ oscillated in the range $\Delta\xi \in$ [-0.62π, -0.43π] with $\Delta\xi_{\text{eff}}$ = -0.56 π, as shown in Fig. 1 (b). The TM amplitude (Fig. 3

(d)) only slightly decreased comparing to that before applying MRMP s.

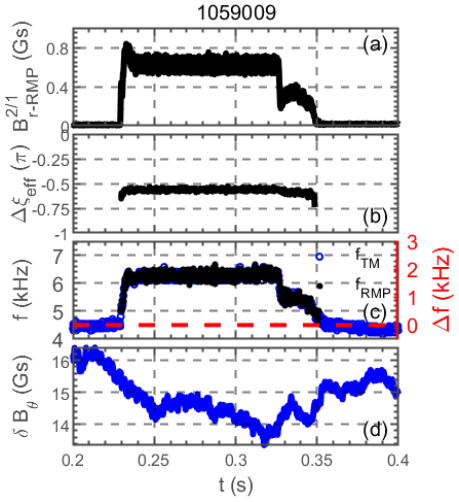

Fig. 3 TM rotation acceleration by MRMP, with $\Delta\xi_{eff}$ = -0.56 π. From top to bottom: the time evolution of (a) the amplitude of the 2/1 component MRMP, (b) the effective phase difference $\Delta\xi_{eff}$ between MRMP and TM, (c) the cycling averaged frequency of TM (blue) and MRMP (black), (d) the amplitude of perturbed poloidal magnetic field measured by Mirnov probes, which represents the TM amplitude.

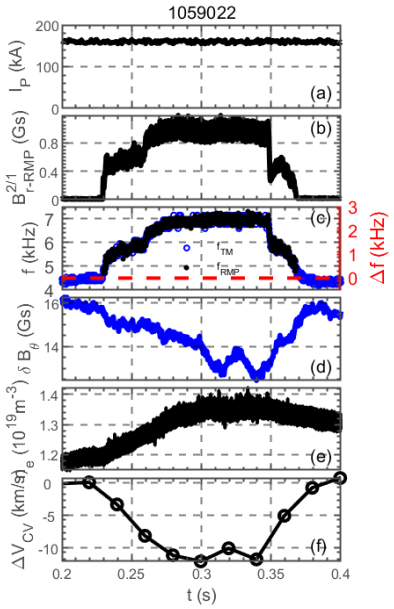

Fig. 4 TM rotation acceleration by MRMP, with $\Delta\xi_{eff}$ = -0.46 π. From top to bottom: the time evolution of (a) the plasma current, (b) the MRMP amplitude of the 2/1 component, (c) the cycling averaged frequency of the TM (blue) and the MRMP (black), (d) the amplitude of perturbed poloidal magnetic field measured by Mirnov probes, which represents the TM amplitude, (e) the line averaged electron density passing through the magnetic axis n_e, (f) the relative change of the C_V toroidal rotation at 0.87 a. The values for the right vertical axis in (c) is the relative variation of TM frequency, Δf, after applying the MRMP.

Another discharge with $\Delta\xi_{eff}$ = -0.46 π is shown in Fig. 4. There were two flattops in the MRMP amplitude, as shown in Fig. 4 (b). When the MRMP amplitude was

increased, the TM frequency increased in a time scale of several rotation periods before it reached a steady value. This might be caused by the change of the plasma rotation velocity profile. When the TM was accelerated, the plasma rotation outside the island would also be accelerated due to the viscous torque. Based on the Electron Cyclotron Emission (ECE) signal, the 2/1 island was located around 22 cm ($r_s \approx 0.86$ a). The change of the edge impurity ion toroidal velocity at r = 0.87 a has been measured by the Edge Radiation Diagnostic (ERD). When the TM rotation increased from 4.3 kHz to 7.0 kHz, the edge impurity ion toroidal velocity changed about -10 km/s, shown in Fig. 4 (f). The line average electron density was increased from 1.2×10^{19}m^{-3} to 1.35×10^{19}m^{-3} (Fig. 4 (e)). When the MRMP was turned off, the edge impurity ion toroidal velocity recovered, and the line averaged electron density decreased to 1.3×10^{19}m^{-3}.

The acceleration of TM rotation depends on the MRMP amplitude, as shown in Fig. 4. The TM frequency difference after and before applying MRMP, $\Delta f = f_{ave} - f_{ave,0}$, is shown in Fig. 5 by black circle points. A linear relationship was found between Δf and the MRMP amplitude. The fitting result, $\Delta f = (2.85 \pm 0.05) B^{2/1}_{r,RMP}$, is shown by the blue line in the Fig. 5.

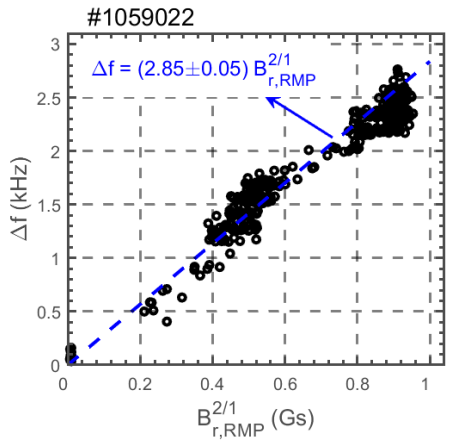

Fig. 5 The variation of TM frequency, Δf, versus the MRMP amplitude, $B^{2/1}_{r,RMP}$ in discharge #1059022. The black circles are obtained from the time evolution of Δf and $B^{2/1}_{r,RMP}$ shown in Fig. 4. The blue dashed line shows a linear fitting to the experimental data.

The impact of the MRMP on the TM also depends on their relative phase. Fig. 5 displays the results for 3 discharges with $\Delta\xi_{eff}$ = -0.59 π, 0.25 π and 0, respectively. With $\Delta\xi_{eff}$ = -0.59π (#1059016, red lines), the MRMP amplitude was ramped up to 0.6 Gs within 6 ms, and f_{TM} was increased from 4.2 kHz to 6.2 kHz. After the MRMP amplitude was ramped down, f_{TM} was reduced to its initial value. With $\Delta\xi_{eff}$ = -0.05 π (#1059014, black lines), the value of f_{TM} was unchanged throughout the discharge. With $\Delta\xi_{eff}$ = 0.25 π (#1058910, blue lines), the MRMP was ramped up to 0.36 Gs for only about 10 ms flattop due to the engineering limit of the power supply system. In this case f_{TM} was decreased from 4.4 kHz to 3.8 kHz (-10%), as expected.

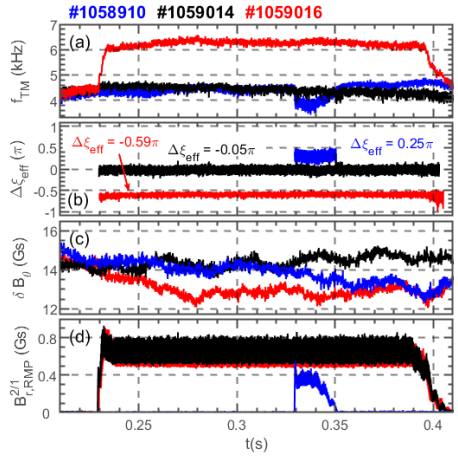

Fig. 6 The impact of MRMP on TM for $\Delta\xi_{eff}$ = -0.59π (#1059016, red lines), $\Delta\xi_{eff}$ = 0.25 π (#1058910, blue lines) and $\Delta\xi_{eff}$ = -0.05 π (#1059014, black lines) region. All the panels have the same meaning as those of Fig. 3, except (a) shows the instantaneous frequency of TM.

Fig. 6 (c) shows the time evolution of the TM amplitude for these three cases. With $\Delta\xi_{eff}$ = -0.59 π (#1059016, red lines), the TM amplitude slightly decreased from t=0.21 s to 0.26 s, but the decreasing rate of TM amplitude was the same before and after the MRMP is applied at 0.23 s. Therefore, the decrease of TM amplitude in this case might not be directly caused by MRMP. With $\Delta\xi_{eff}$ = -0.05 π (#1059014, black lines), the MRMP has no significant destabilization effect on the mode amplitude, as expected for a small MRMP amplitude and a large island.

The change of TM rotation frequency by MRMP is displayed in Fig. 7 as a function of the relative phase. Since the MRMP amplitude also influences the value of Δf, only the data with the MRMP amplitude in the range of [0.56 Gs, 0.64 Gs] from 9 discharges are shown by the black circles. The fitting of the data, Δf = -(1.95 ± 0.2) sin ($\Delta\xi_{eff}$), is shown by the black dashed line. These results confirm experimentally that the TM acceleration by MRMP has the highest efficiency for $\Delta\xi_{eff}$ = -0.5 π. As there is no result with the MRMP amplitude around 0.6 Gs for $\Delta\xi_{eff}$ > 0, the result from discharge #1058910 with $B^{2/1}_{r,\,RMP}$ = 0.39 Gs and $\Delta\xi_{eff}$ = 0.25π is shown in Fig. 7 by the blue triangle. It is scaled to $B^{2/1}_{r,\,RMP}$ = 0.64 Gs by assuming a linear dependence of Δf on $B^{2/1}_{r,\,RMP}$, as shown by the blue square.

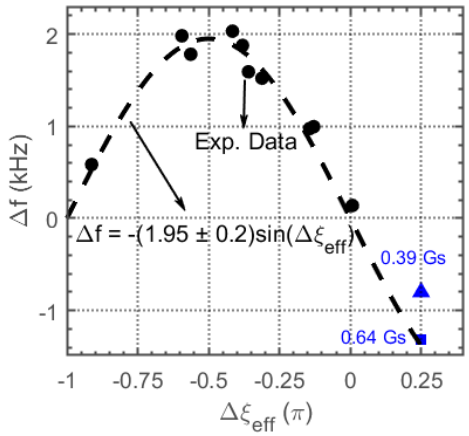

Fig. 7 Change of TM frequency by MRMP, Δf, versus $\Delta\xi_{eff}$. The black circles are

*obtained from 9 discharges with the MRMP amplitude in the range of [0.56 Gs, 0.64 Gs]. A fitting to these data is shown by the black dashed line with Δf = -1.95*sin($\Delta\xi_{eff}$). The blue triangle is for the case with $B^{2/1}_{r,RMP}$ = 0.39 Gs and $\Delta\xi_{eff}$ = 0.25π, and the blue square is scaled value for $B^{2/1}_{r,RMP}$ = 0.64 Gs by assuming a linear dependence of Δf on $B^{2/1}_{r}$.*

The blue circles in Fig. 8 display the experimental data for the relationship between Δf and -sin($\Delta\xi_{eff}$) $B^{2/1}_{r,RMP}$. A linear fitting of the experimental data gives, Δf = (-2.95 ± 0.25) * $B^{2/1}_{r,RMP}$ * sin($\Delta\xi_{eff}$). The applied EM torque has to balance with the plasma viscous torque, which is proportional to Δf, if assuming no significant change in the plasma viscosity [18].

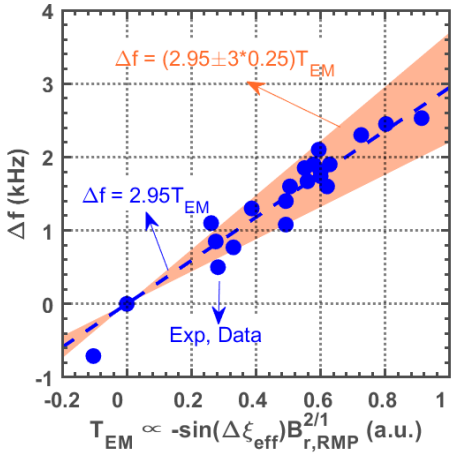

Fig. 8 The relationship between the variation of TM frequency, Δf, and the electromagnetic torque applied by MRMP, $T_{EM} \propto$ -sin ($\Delta\xi_{eff}$) $B^{2/1}_{r,RMP}$. The fitting (blue dashed line) shows a linear dependence of Δf on T_{EM}.

The MRMP is more effective in accelerating TM than with the rotating RMP. The dynamic effect of RMP on the TM relies on the phased difference between them, $\Delta\xi$. Before the TM locked on the rotating RMP, the $\Delta\xi$ keep increases/decreases with time and the rotating RMP alternately contributes an accelerating or decelerating torque on the TM. The net dynamic effect of rotating RMP decreases with the increase of the frequency difference between RMP and TM. As a result, it's difficult to accelerate TM by the rotating RMP with a frequency difference 2.5 kHz in J-TEXT [15]. Applying the MRMP, the $\Delta\xi$ oscillated in a small region around the $\Delta\xi_{eff}$. Applying MRMP, $\Delta\xi$ oscillated with in a small region and the MRMP only contributes an accelerating torque on the TM. The TM could be accelerated from 4.3 kHz to 7 kHz (> 60 %) with a small MRMP. Hence, the MRMP is more effective in accelerating TM than with the rotating RMP.

4. Discussion and Conclusion

The conventional idea to suppress the TM by feedback RMP is to apply the RMP in the opposite phase of the mode [17]. However, this method requires larger RMP amplitude to suppress a larger island substantially. It is found in our experiments that a small MRMP, ~0.6Gs ~ 4*10^{-5} toroidal field, has little effect on the mode amplitude. Nevertheless, the MRMP is very effective to speed up the island rotation when phased

with $\Delta\xi_{eff}$ ~ 3π/2 via feedback control, accelerating the rotation from 4.3 kHz to 7.0 kHz. To speed up the island rotation from/to a lower mode frequency, the required RMP amplitude is smaller due to a smaller the eddy current in the wall, and the required power supply would be much lower due to both a smaller RMP amplitude and a lower frequency. As the applied EM torque from RMPs is proportional to the square of the Alfven velocity, the required normalized (to toroidal field) MRMP amplitude for speeding up the island rotation is smaller for a fusion reactor than that for existing tokamaks [9], indicating a possible efficient method for avoiding mode locking in a fusion reactor. To simultaneously accelerate and suppress the TM, however, large MRMP applied with a relative phase $\pi < \Delta\xi < 3\pi/2$ would be required [20].

In conclusion, the acceleration of magnetic island rotation by MRMP is studied experimentally via feedback control, to have different relative phase between the island and the RMP. The relative phase is found to be important for the island acceleration, being most effective for the relative phase about -π/2. The island rotation frequency is increased by a few kHz for the optimized relative phase by a small MRMP. The accelerating effects is also proportional to the MRMP amplitude.

Acknowledgement

This work is supported by the National Key R&D Program of China under Grant No. 2018YFE0309101, the National Natural Science Foundation of China (Contract No. 12075096, No. 12047526 and No. 51821005) and "the Fundamental Research Funds for the Central Universities" under Grant No. 2020kfyXJJS003.

Reference

[1] R. J. La Haye, *et al* 2006 *Physics of Plasmas* **13** 055501
[2] R. J. La Haye, *et al* 2000 *Physics of Plasmas* 7 3349
[3] R.C. Wolf, *et al* 2005 *Nucl. Fusion* **45** 1700
[4] M.F.F. Nave, J.A. Wesson 1990 *Nucl. Fusion* **30** 2575
[5] J. K. Park, *et al* 2007 *Phys. Rev. Lett.* **99** 195003
[6] X. Wang, *et al* 1997 *Physics of Plasmas* **4** 748
[7] R. Sweeney, *e t al* 2018 *Nucl. Fusion* **58** 056022
[8] R. Sweeney. *et al* 2016 *Nucl. Fusion* **57** 016019
[9] Q. Yu, *et al* 2008 *Nucl. Fusion* **48** 065004
[10] H. Zohm *et al* 1999 *Nucl. Fusion* **39** 577
[11] R. Prater *et al* 2003 *Nucl. Fusion* **43** 11282003
[12] E. Westerhof, *et al* 2007 *Nucl. Fusion* **47** 85
[13] P.C. De Vries, *et al* 2016 *Nucl. Fusion* **56** 026007
[14] E.J. Strait, *et al* 2019 *Nucl. Fusion* **59** 112012
[15] B. Rao, *et al* 2013 *Plasma Phys. Control. Fusion* **55** 122001
[16] D. Li, *et al* 2020 *Nucl. Fusion* **60** 056022
[17] G.A. Navratil, *et al* 1998 *Phys. Plasmas* **5** 1855
[18] K. Bol *et al* 1975 in Proceeding of the 5th IAEA International Conference on Plasma Physics and Controlled Nuclear Fusion Research (IAEA, Vienna), Vol. 1, p. 83

[19] D.L. Nadle, *et al* 2000 *Nucl. Fusion* **40** 1791
[20] Q. Hu, Q. Yu 2016 *Nuclear Fusion* **56** 034001
[21] B. Rao, et al 2014 *Fusion Engineering and Design* **89** 378
[22] W. Zheng, *et al* 2018 *IEEE Transactions on Nuclear Science*, **65** 2344.
[23] M. Li, *et al* 2019 *Fusion Engineering and Design* **146** 2130
[24] Y. Liang, *et al* 2019 *Nucl. Fusion* **59** 112016
[25] Y. Ding, *et al* 2018 *Plasma Sci. Technol.* **20** 125101
[26] L. Frassinetti, *et al* 2010 *Nucl. Fusion* **50** 035005
[27] T.C. Hender, *et al* 1992 Nucl. Fusion32 2091
[28] Q. Hu, *et al* 2013 *Phys. Plasmas* **20** 092502
[29] R. Fitzpatrick 1993 *Nucl. Fusion* **33** 1049
[30] N. Wang, *et al* 2019 *Nucl. Fusion* **59** 054002
[31] W. Zheng, *et al* 2018 *IEEE Transactions on Nuclear Science*, **65** 2344.
[32] B. Rao, *et al* 2016 *Review of Scientific Instruments* **87** 1153